Research Article **Rev. Cong. Sci. Technol., Vol. 5, No. 2, pp. 717-735 (2026)**

OPEN ACCESS

Revue Congolaise des Sciences & Technologies

ISSN: 2959-202X (Online); 2960-2629 (Print)

https://www.csnrdc.net/

REVUE CONGOLAISE DES SCIENCES ET TECHNOLOGIES

Test of Regeneration of used Engine oils by Percolation using Activated Red Clay

[Essai de Régénération des Huiles Moteurs Usagées par Percolation à l'aide d'Argile Rouge activée]

Ismael Kabuya Mulumba[1], Hermine Kitu Malengila[1], Théodore Kazadi Kashishi[1], Arsene Kayeye Muabu[1], Naomie Mpandu Bolangongo[1], Christiane Nsende Ngoyi[2], Joachim Muyumba[1], Emmanuel Kalonji Kapuya[1], Jeffrey Mihala Kamwiziku[1], Michee Kazadi Mputu[2] Kalulu Muzele Taba[1] & Joséphine Kankolongo Ntumba[1*]

[1] Department of Chemistry, Faculty of Sciences, University of Kinshasa, Kinshasa, RD Congo

[2] Department of Environment, Faculty of Sciences, University of Kinshasa, Kinshasa, RD Congo

Abstract

Used lubricating oils, after being drained, end up being released into the environment. They have an impact on both humans and the environment if they are not properly disposed of and managed. Indeed, environmental pollution is one of the problems facing humanity today. There are several factors that exacerbate environmental pollution, including the uncontrolled disposal of used motor oils. The need for an environment free from all toxic threats is constantly growing in society. The present work aims to regenerate used lubricating oils from activated clay filter discs. The results show that certain parameters such as density, kinematic viscosity, viscosity index, flash point, and pour point underwent changes, suggesting partial regeneration of the used oil. However, the color of the treated oil remained unchanged.

Mots-clés: Used lubricating oils, pollution, regeneration, activated clay filter discs and parameters.

Résumé

Les huiles lubrifiantes usagées, après leur vidange, sont souvent rejetées dans l'environnement. Elles ont un impact à la fois sur la santé humaine et sur l'environnement lorsqu'elles ne sont pas correctement éliminées et gérées. En effet, la pollution environnementale constitue aujourd'hui l'un des problèmes majeurs auxquels l'humanité est confrontée. Plusieurs facteurs aggravent cette pollution, notamment le rejet incontrôlé des huiles moteurs usagées. Le besoin d'un environnement exempt de toute menace toxique ne cesse de croître au sein de la société. Le présent travail vise à régénérer les huiles lubrifiantes usagées à l'aide de disques filtrants en argile activée. Les résultats montrent que certains paramètres, tels que la densité, la viscosité cinématique, l'indice de viscosité, le point d'éclair et le point d'écoulement, ont subi des modifications, indiquant une régénération partielle de l'huile usagée. Cependant, la couleur de l'huile traitée est restée inchangée.

Keywords : Huiles lubrifiantes usagées, pollution, régénération, disques filtrants en argile activée, paramètres

*Auteur correspondant : Joséphine Kankolongo Ntumba, (josephine.ntumba@unikin.ac.cd). Tél. : (+243) 854 704 596

https://orcid.org/0009-0003-1914-3741 ; Reçu le 31/03/2026 ; Révisé le 24/04/2026 ; Accepté le 19/05/2026

DOI : https://doi.org/10.59228/rcst.026.v5.i2.280

Copyright: ©2026 Mulumba et al. This is an open-access article distributed under the terms of the Creative Commons Attribution-NonCommercial-ShareAlike 4.0 International License (CC-BY-NC-SA 4.0), which permits unrestricted use, distribution, and reproduction in any medium, provided the original author and source are credited.

1. Introduction

Lubricating oils play a fundamental role in the proper functioning of internal combustion engines. Their performance depends on several key physicochemical properties, including viscosity, density, and thermal stability. Over time, however, these oils gradually become contaminated with metallic particles, combustion residues, and degradation by-products. This accumulation progressively alters their performance and significantly shortens their service life. Once degraded beyond acceptable limits, such oils are typically drained and, in many cases, disposed of improperly, leading to considerable environmental pollution (Cabrera Escobar et al., 2026; Sarkar et al., 2023).

Used lubricating oils (ULOs) therefore represent one of the major sources of hazardous liquid waste worldwide. When discharged without proper control into soils or aquatic environments, they cause persistent contamination, induce toxic effects, and disrupt ecosystem balance (Cabrera Escobar et al., 2026). Addressing this issue requires the development and implementation of sustainable recovery and regeneration strategies. These approaches aim not only to restore the functional properties of degraded oils but also to limit their overall environmental impact (Negasa et al., 2025; Mishra et al., 2025).

Among the various available techniques, adsorption-based regeneration stands out as a particularly promising approach. Its appeal lies in its relative simplicity, economic feasibility, and operational flexibility. In this context, activated clays have attracted increasing attention as effective adsorbents. They are abundant, inexpensive, and exhibit enhanced adsorption capacity following chemical modification. Acid activation, in particular, increases the specific surface area of clays and alters their surface chemistry, thereby improving their ability to capture both polar and non-polar contaminants (Wang et al., 2019; Sabadash, 2024). Recent studies further indicate that the use of natural or modified sorbents can substantially reduce hydrocarbon pollutants while improving key oil quality parameters (Sarkar et al., 2024; Negasa et al., 2025).

The present study aims to investigate the adsorption mechanisms of impurities in used lubricating oils using acid-activated red clay. The evaluation of oil properties is conducted in accordance with ASTM standards, including D445 (kinematic viscosity), D4052 (density), D92 (flash point), and D97 (pour point). The working hypothesis is that acid activation enhances the physicochemical properties of the clay, thereby enabling the partial regeneration of used oils. This research contributes to efforts to reduce environmental pollution, promote recycling practices, and valorize locally available clay materials as low-cost adsorbents for oil treatment.

2. Material and methods

The raw clay samples used in this study were collected from the LODI deposit located in Kimwenza Gare, within the Mont Ngafula district of Kinshasa (Democratic Republic of Congo). These materials were first subjected to activation procedures and subsequently characterized in order to determine both their mineralogical composition and key physicochemical properties. This characterization step provided essential insights into the nature of the clays and their potential suitability for adsorption-based applications.

Following activation, the clays were applied to the treatment of used motor oils, where they functioned as adsorbents for the removal of impurities and degradation products. The regeneration process was carried out through direct contact between the clay and the oil samples, enabling adsorption mechanisms to take place under controlled experimental conditions.

A comparative analysis was then conducted on fresh, used, and treated lubricating oils to assess the effectiveness of the clay-based treatment. Several parameters were evaluated, including density, viscosity, acidity, and color, all measured in accordance with standardized methods (ASTM and AFNOR).

2.1. Materials, methods and equipment

The experimental work was conducted using standard laboratory equipment and analytical instruments. Volumetric flasks and three-neck round-bottom flasks were employed for solution preparation and reaction setups, while a hot plate with a magnetic stirrer ensured homogeneous mixing. Precise measurements were obtained using an analytical balance and graduated pipettes, and temperature control was maintained with a water bath and thermometers.

Magnetic stir bars facilitated continuous agitation, and filtration was performed with 150 mm

filter papers, Büchner funnels, and vacuum flasks connected to a rotary evaporator. Condensers were used for reflux operations, while pH measurements were taken with a calibrated pH meter. Additional glassware included Pyrex beakers, funnels, wash bottles, and graduated cylinders.

Thermal treatments were carried out in drying ovens, and platinum crucibles were used for calcination procedures. Samples were handled with spatulas and secured using metal clamps. A desiccator was employed to preserve activated materials under controlled humidity, and sieves were used to obtain uniform particle sizes.

The reagents used in this study included concentrated sulfuric acid (H_2SO_4, 96%), distilled water (H_2O), sodium chloride (NaCl), sodium hydroxide (NaOH), pre-melted lithium borate flux, and hydrochloric acid (HCl). These chemicals were essential for activation, neutralization, and analytical preparation.

Analytical characterization was performed using specialized equipment. Structural and compositional analyses were carried out with a diffractometer and an X-ray fluorescence spectrometer, while particle size distribution was determined using a particle size analyzer. Physicochemical parameters were measured with a densitometer and a calibrated pH meter. Viscosity was assessed using a capillary viscometer, ensuring precise evaluation of the flow properties of the lubricating oils before and after treatment

2.2. Methods, characterization and analyses

2.2.1. Preparation of activated clay

a. Pretreatment of clays

Before activating the clay, we pretreated it as follows:

- Weigh out 125g of clay;
- Oven dry for 24 hours at a temperature of approximately 105°C;
- Grind using a grinder;
- Sift through a sieve.

b. Chemical activation

3N H2SO4 solution was prepared from a 96% H2SO4 solution as follows: in a one - liter volumetric flask, we mixed 83.3 mL of the 96 % acid solution and 916.7 mL of water.

The clay was then activated by placing 125 g of raw clay and 375 mL of 3N H_2SO_4 in a 500 mL three-necked flask equipped with a condenser and thermometer.

The mixture was heated to 70 °C for 4 hours with stirring. After this period, the mixture was allowed to settle and then filtered under vacuum. Following several washes with distilled water (to remove excess acid until a neutral pH was reached), the acidified clay was dried in an oven, then ground and sieved. The activated clay was stored away from moisture for later use (Boudouara, 2021).

2.2.2. Physicochemical analyses

a. Particle Size

Particle size analysis was performed using a column containing sieves with the following dimensions: 2 mm, 1 mm, 500 µm, 250 µm, 125 µm, and 63 µm. The sieves were stacked in descending order of size, so that the openings decreased in size from top to bottom of the column. A lid was placed at the top of the column to prevent any loss of fine particles during sieving.

Operating procedure (Amirouche, 2011):

Weigh out a quantity (P0) of the crushed and oven-dried clay at 105°C, and pour it into the top of the column. Then, vibrate the column using the electric sieve shaker for 5 minutes.

The weight of the material passing through a given sieve is called the sieve weight (T), while the weight of the material retained by the same sieve is called the oversize. (P). The sieve residue (RT) is calculated according to the formula:

$$\mathbf{RT}(\%) = \frac{\mathbf{P}}{\mathbf{P0}} \times 100$$

The sieving rate (cumulative passing) = T (%) = 100 – RT

b. Zero Charge Point (NCP)

The pH of the zero-charge point corresponds to the pH value at which the net charge of the solid surface is zero. This parameter is very important in adsorption phenomena, especially when electrostatic forces are involved in these mechanisms.

Operating procedure:

The experimental protocol for determining the PCN is as follows:

50 mg of clay are added to 20 ml of NaCl (0.1M) solution at different pH levels, ranging from 2 to 12. The pH is adjusted by adding HCl and/or NaOH at a concentration of 0.01M.

The clay-containing solutions are stirred for 24 hours at a speed of 300 rpm.

After this period, the final pH of the solutions is measured.

First, we plot the curve of the final pH as a function of the initial pH. Second, we plot the line representing the initial pH as a function of the initial

pH. The point of intersection between these two curves corresponds to the PCN of our clay (Zahaf, 2017).

c. Hydrogen potential

Operating procedure:

Weigh out 5g of clay, immerse it in 100 ml of distilled water, and stir the mixture for 5 minutes. After one hour of resting, measure the pH of the supernatant liquid using a pH meter. We used an InoLab brand pH meter (Fouzia, 2015).

d. Moisture Content

Moisture content is defined as the amount of water contained in a substance, equivalent to the difference between the mass of the fresh sample (mi) and the mass of the dry sample (mf). The procedure consists of drying a clay sample in an oven at 110 °C for one hour, then cooling it in a desiccator before reweighing. This oven-drying method is widely recognized as a reliable technique for determining soil moisture content (Khole, Tupe, & Sayyad, 2023).

Operating procedure:

Place a sample of approximately 3g of clay (m _i) in an oven. Dry for one hour at a temperature set between 105°C and 110°C. Place the dried sample in a desiccator and reweigh it cold (m_f). The moisture content is calculated using the following formula:

$$\mathbf{MC}(\%) = \frac{\mathbf{mi - mf}}{\mathbf{mi}} \times \mathbf{100}$$

e. Loss in the fire

Loss on ignition (LOI) analysis provides an indication of the organic matter content and organic carbon content in a sample. The operating procedure is as follows: weigh the mass of the empty platinum crucible (m0) in grams, then tare the mass of the empty crucible on the balance and weigh the mass of the sample (mech) in grams in this crucible, in order to find P1=m0+mech. Place the crucible containing the sample (P1) in a furnace at 1050 °C for 1 hour for loss on ignition. After ignition, cool the platinum crucible in the desiccator and then weigh again to obtain P2. The loss due to ignition is determined by the following relationship:The loss due to ignition is determined by the following relationship:

$$\mathbf{LOI} = \frac{\mathbf{P1-P2}}{\mathbf{mech}} \mathbf{x\ 100}$$

This method is widely recognized for estimating organic matter in soils and sediments (Heiri, Lotter, & Lemcke, 2001; Zhang et al, 2022).

f. Thermogravimetry

Thermogravimetry provides, as a function of temperature, the mass loss experienced by the sample during heating. It allows for the localization of clay dehydration temperatures as well as the decomposition of intercalated species. It also allows for the quantitative determination of decomposition phenomena: hydrates, carbonates, oxalates, etc. It contributes to the identification of clay minerals: departure of different types of water, organic matter, etc. This method has been highlighted in earlier studies (Ravelomanantsoa, 2015) and confirmed by recent research (Lo Dico et al., 2024).

2.2.3. Characterization of clays

a. Chemical composition

a.1. Method: XRF (X-ray fluorescence):

This analysis is crucial for determining the oxide composition of clay. X-ray fluorescence (XRF) spectrometry enables both qualitative and quantitative assessment of chemical constituents.

a.2. Principle:

The method is based on irradiating the sample with an X-ray beam, which induces the emission of secondary X-rays characteristic of the elements present. This principle has been described in earlier work (Derafa, 2014) and further supported by recent studies applying XRF to clay mineral characterization (Zhou et al., 2021).

a.3. Analysis and equipment:

The X-ray fluorescence spectrometer used is a BRUKER S8 TIGER. (available in the analysis laboratory of the industrial cement production company, CILU, in Lukala).

- Weigh 0.9 g of the sample after calcination (loss on ignition) and weigh 6.3 g of flux (pre-melted lithium borate flux) and put them in a platinum crucible;
- Place the crucible in the furnace at a temperature of approximately 1000°C for melting;
- After melting, remove the crucible from the oven and pour the molten liquid into a mold;
- Allow to cool;
- Remove the pearl (see appendix) from the mold; it will then be placed in the apparatus for analysis.

(crystal made from molten clay).

b. Mineralogical composition

b.1. Method: XDF (X-ray diffraction)

X-ray diffraction is a widely used technique for identifying the structure and nature of crystalline materials. It is particularly applied to solids such as rocks, minerals, pigments, and clays, which exhibit a periodic and ordered arrangement of atoms in three-dimensional lattice planes. This method is essential for determining clay mineralogy and associated impurities (Zhou et al., 2021; Lo Dico et al., 2024).

b.2. Principle

The technique consists of irradiating the sample with an X-ray beam and recording the intensity of the diffracted rays (figure 1). The scattering phenomenon results from the interaction between the incident beam and the crystal lattice. The relationship between the diffraction angle and the interplanar spacing of atoms is expressed by Bragg's law:

$n\lambda=2d\sin\theta$

Where:

- λ = wavelength (Å)
- d = interplanar spacing
- θ = diffraction angle(°)

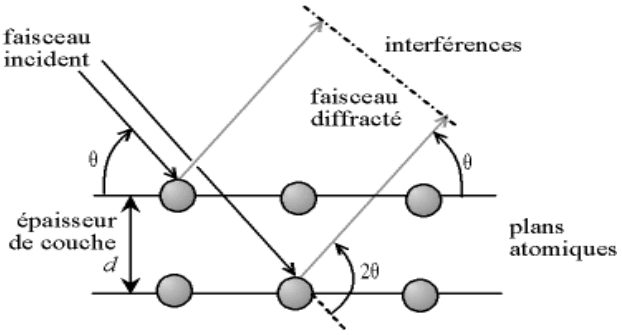

Figure 1. XRD principle

b.3. Analysis and equipment

The mineralogical analyses were performed in the laboratory of the CILU industrial cement production company using a BRUKER D2-PHASER diffractometer, a modern instrument widely employed for X-ray diffraction studies of crystalline materials.

- Operating procedure

The powdered samples were carefully pressed into a support to ensure homogeneity, then mounted in a suitable sample holder. Each prepared sample was subjected to an X-ray beam, which was diffracted by the lattice planes of the crystalline phases. The resulting diffraction patterns were recorded and analyzed to determine the mineralogical composition. (Zhou et al., 2021; Lo Dico et al., 2024).

2.2.4. Manufacturing of filter discs

This stage of the work was conducted in the mechanical workshop of I Engineering RDC. The fabrication of chemically activated clay filter discs followed a series of successive steps. First, a clay paste was prepared by adding water and manually kneading the material until a homogeneous and sufficiently malleable consistency was obtained. The paste was then molded using a PVC formwork (12 cm in diameter and 5 cm in thickness) to produce discs with the desired geometry. Small perforations were subsequently introduced across the surface of the discs to facilitate fluid flow through the filtration medium. Finally, the discs were dried under sunlight until they reached adequate rigidity and structural consistency. Comparable fabrication approaches combining paste preparation, shaping, perforation, and drying are widely reported in the production of porous ceramic and clay-based materials for filtration and adsorption applications (Grema et al., 2021). In this context, perforation was specifically intended to enhance hydraulic conductivity and promote a more uniform distribution of the fluid within the medium, thereby limiting excessive pressure buildup inside the clay matrix.

The use of clay-based filter discs was motivated by the well-established adsorption properties of activated clays. These materials are characterized by a high specific surface area, a layered porous structure, and significant ion-exchange capacity. Such features favor the retention of a wide range of contaminants typically present in used lubricating oils, including polar compounds, oxidation by-products, sludge precursors, and suspended particles (Anisuzzaman & Jumadil, 2024; Isam et al., 2021). Numerous studies indexed in Scopus and Web of Science have highlighted the effectiveness of acid-activated natural clays for the purification and regeneration of industrial and waste oils, emphasizing their low cost, environmental compatibility, and strong adsorption performance (Biruk et al., 2022; Osman et al., 2021; Dodoo et al., 2023).

The disc configuration was initially selected because it provides a compact and relatively simple filtration medium, with low production costs and straightforward integration into small-scale treatment systems. Similar clay-based porous structures have been investigated in various adsorption and filtration contexts due to their accessibility and suitability for localized treatment applications (Low-Cost Antibacterial Ceramic Water Filters Project, 2024;

Grema et al., 2021). However, experimental observations revealed several limitations when the system was exposed to complex mixtures containing heavy molecular compounds, such as high-molecular-weight organics, humic-like substances, and clay colloids.

In practice, several drawbacks became apparent. Rapid pore clogging was frequently observed, leading to obstruction of the filtration pathways (Sorrentino et al., 2025). In addition, the discs exhibited deformation and, in some cases, rupture when subjected to hydraulic pressure. This fragility necessitated frequent replacement, which increased both operational variability and treatment costs. There was also a risk of bypass leakage when the applied pressure exceeded the mechanical resistance of the discs, further compromising system reliability.

The drying stage contributed to these mechanical weaknesses. Shrinkage and uneven moisture distribution within the clay matrix generated structural heterogeneities that reduced overall integrity. Previous studies have shown that uncontrolled drying conditions can induce cracking, shrinkage, and increased fragility in clay-based porous materials, thereby negatively affecting both their mechanical resistance and filtration performance (Isam et al., 2021; Low-Cost Antibacterial Ceramic Water Filters Project, 2024). In the present case, such effects likely facilitated crack formation during continuous filtration and reduced the durability of the discs.

To address these limitations, a packed column filtration system was subsequently adopted. The transition from disc-based filtration to column adsorption was guided by both practical observations and established findings in the adsorption literature. Column systems offer a more homogeneous distribution of flow, which limits localized clogging phenomena (Sorrentino et al., 2025; Isam et al., 2021). They also allow the treatment of larger volumes and provide improved retention of heavy molecular fractions (Dodoo et al., 2023). In addition, they exhibit superior mechanical stability, enabling operation under higher pressures without structural failure. Another advantage lies in their flexibility: a wide range of adsorbents including activated clays, silica-based materials, and ion-exchange resins can be incorporated depending on the targeted contaminants (Isam et al., 2021; Boudouara, 2021). Maintenance is also simplified, as the adsorbent bed can be replaced or regenerated without dismantling the entire system (Isam et al., 2021).

More broadly, adsorption columns are widely used in chemical separation and wastewater treatment because they enhance contact between the fluid phase and the active sites of the adsorbent. In a packed bed configuration, continuous interaction between the oil and the sorbent promotes more efficient mass transfer compared with compact filtration media such as discs. The increased residence time within the column further improves adsorption efficiency and contaminant removal (Isam et al., 2021; Dodoo et al., 2023).

Although the present study primarily aimed to assess the feasibility of using activated clay for the regeneration of lubricating oils, the experimental conditions were defined based on procedures commonly reported for fixed-bed column systems and acid-activated clay treatments (Anisuzzaman & Jumadil, 2024; Dodoo et al., 2023; Osman et al., 2021). Further optimization particularly with respect to particle size, flow rate, contact time, and bed height could significantly enhance both the efficiency and reproducibility of the process.

At this stage, the work should be regarded as a preliminary feasibility study. Additional investigations are required to fully establish the industrial relevance of the proposed system. These should include detailed analyses of adsorption kinetics, breakthrough behavior, process optimization, and comparisons with conventional adsorbents (Isam et al., 2023; Dodoo et al., 2023; Sorrentino et al., 2025).

2.2.5. Treatment of used lubricating oils

Used oil samples were collected from the telecommunications company I Engineering DRC. These oils originated from generators supplying power to telecommunications antennas. As part of standard maintenance procedures, they were systematically recovered during oil changes and stored in dedicated tanks, ensuring appropriate waste management.

For comparative purposes, a new SAE 40 lubricating oil was used as a reference alongside the used and treated samples. This comparison made it possible to assess the effectiveness of the clay-based filtration process. The selection of SAE 40 oil was guided by its widespread industrial use and ready availability (Ghafar et al., 2020).

A filtration system was designed using a PVC column, within which two clay filter discs were positioned in parallel and separated by a 2 cm Hollow

spacing to promote fluid circulation. The setup consisted of a pre-filtration tank fitted with cotton fabric, a filtration unit, a treated oil recovery tank, and a motor-driven pump to ensure continuous flow. The use of PVC columns for housing clay-based adsorbents is well documented in adsorption systems and is recognized for its practicality and operational efficiency (Khan et al., 2023; Dawood et al., 2025).

a. Filtration procedure

The filtration process began by introducing the used oil into the pre-filtration tank connected to the system. The pump was then activated to circulate the oil through the filter, allowing the treated oil to be collected in the recovery tank. This cycle was repeated several times until the adsorbent material reached saturation.

The initial objective was to regenerate used lubricating oils using activated clay discs. Although these discs were successfully produced, they exhibited significant mechanical fragility, breaking both during and after the drying stage. This weakness, combined with pore clogging under the presence of heavy molecular compounds (Sorrentino et al., 2025), led to a reconsideration of the experimental approach.

As a result, the system was adapted to a packed-column configuration, operating according to principles comparable to column chromatography, where separation occurs through adsorption onto a powdered clay matrix (Madani, 2008). The revised procedure was implemented as follows: 200 g of clay were introduced into the column; 100 mL of used oil were then added; an external force, generated by a motor pump, was applied to drive the oil through the adsorbent bed; the process was repeated four times to enhance treatment efficiency; finally, the regenerated oil was collected and stored in polyethylene containers.

2.2.6. Physicochemical analyses of oil samples

After processing, the samples are placed in polyethylene bottles, labeled, and then sent to the quality control laboratory of the company SEP-CONGO.

The following analyses are performed: color, kinematic viscosity, density, viscosity index, water content, pour point, flash point, and acidity index. These analyses are carried out in accordance with ASTM international standards.

a. The color

It is determined according to the ASTM D1500 standard, where samples are subjected to comparative visual analysis on a color scale (figure 2) (Amrane et al., 2017).

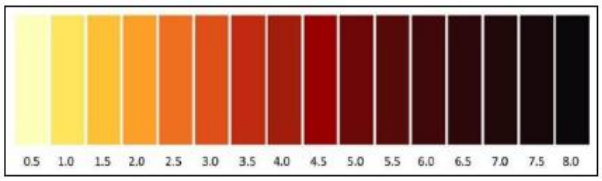

Figure 2. Color scale

b. Kinematic viscosity

Kinematic viscosity is determined experimentally by measuring the time it takes for the fluid to flow through a capillary under the influence of gravity. This measurement is performed using a capillary viscometer at 40°C and 100°C according to ASTM D445 (Armioni et al., 2024).

c. Viscosity index

This property is determined as a function of kinematic viscosity at 40°C and at 100°C according to ASTM D2270 (Touir et al., 2019).

d. The density

This parameter is determined at 15°C using a densimeter according to the ASTM D4052 standard (Armioni et al., 2024).

e. The flash point

The Cleveland brand device is used to measure the flash point according to the ASTM D92 standard (Makaoui, 2020).

f. The pour point

It is measured according to ASTM D97 standard (Bennoui et al., 2021).

3. Results and discussion

3.1. Physicochemical analyses of clays (raw and activated)

3.1.1. Particle size

The results of the particle size analysis carried out on the clays are presented in table I.

Table I. Particle size analysis results

Dimensions (mm and µm)	Rejected by sieve (%)	Cumulative passersby (%)
2mm	0.017	99,983
1mm	0.0036	99.9964
500 µm	1.1	98.9
250 µm	43.57	56, 43
125 µm	32.89	67.11
63 µm	17.25	82.75
< 63 µm	4.9	95.1

figure 3 represents the particle size distribution curve as a function of grain diameter (sieve pore size) and cumulative passing.

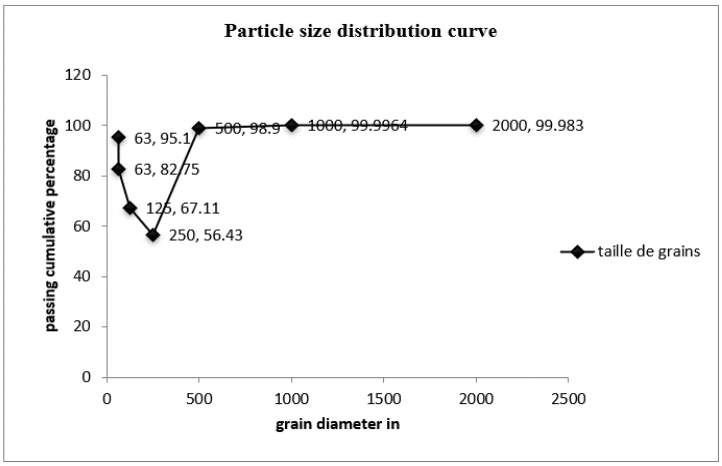

Figure 3. Particle size distribution curve

We observe that the clay fraction characterized by a diameter less than 63 µm constitutes 95.1% by mass of the clay sample. This high composition of fine particles gives clay unique physico-chemical properties, such as its capacity to adsorb ions and molecules, essential in applications such as water retention in agricultural soils or the decontamination of polluted soils (Demirbas, 2009).

Amirouche (2011) found that the clay fraction, characterized by a diameter less than 63 µm, constituted approximately 40% by mass of the clay sample. The remainder of the sample consisted of fine sand according to the ASTM classification (table II).

Granule	Fine clays	Silts and clays	Fine sands	Medium sands	Coarse sand	Fine gravel
Diameter (mm)	0-0.053	0.053-0.063	0.07 5-0.5	0.5-2	2-15	14-20

Gorączko & Topoliński (2020), using laser diffraction and hydrometric analyses, showed that Neogene clays are predominantly composed of particles smaller than 63 µm. This fine granulometric distribution directly accounts for their high adsorption capacity as well as their role in soil structuring. Such methodological rigor strengthens the alignment of our results with those reported in the international literature.

b. Loss on ignition (LOI) and thermogravimetry (TG)

The results of loss on ignition and thermogravimetry of raw and activated clays are given in table III.

Table III. LOI and TG Results

Name	Test method (standards)	Unit	Raw clay (AB)	Activated clay (AA)
LOI 1050°C	DIN EN 196-2:2013	%	5.16	4.40
TG - LOI 70°C-210°C	DIN EN 196-2:2013	%	0.70	0.70
TG - LOI 390°C-630°C	DIN EN 196-2:2013	%	4.50	3.80
TG OH Kaolinite / H_2O Clay	DIN EN 196-2:2013	%	6.70	5.30
TG Kaolinite Content	DIN EN 196-2:2013	%	32.00	27.50

The data presented in this table indicate a relatively low loss on ignition, which can be attributed to several concurrent processes. These include the removal of constitution water, the decomposition of associated minerals such as carbonates, and the combustion of organic matter present in the samples (Bessaha, 2016).

The mass loss observed in samples AB and AA was examined to evaluate the thermal stability of the clays, supported by thermogravimetric analysis as a function of temperature. In the temperature range of 70°C to 210°C, both samples exhibited a mass loss of 0.70%, corresponding to the release of physically bound moisture. This step is particularly important, as moisture content directly affects the plasticity and shrinkage behavior of clays during thermal treatment.

Between 390°C and 630°C, additional mass losses of 4.50% for sample AB and 3.80% for sample AA were recorded. These losses are attributed to the release of adsorbed and interlayer water. This stage of thermal decomposition reflects the presence of water molecules associated with the internal structure of the clay minerals, providing valuable insight into their behavior under heat treatment and their potential performance in industrial applications.

At higher temperatures, further mass losses of 6.70% for sample AB and 5.30% for sample AA were observed. These values correspond to the irreversible dehydroxylation of kaolinite, a key transformation in clay mineralogy that significantly alters both structure and physicochemical properties (Derafa, 2014). This process has been extensively documented: Madejová et al. (2006), using infrared spectroscopy and thermogravimetric analysis, demonstrated that dehydroxylation leads to substantial structural reorganization, notably the formation of metakaolinite, with consequential changes in adsorption behavior.

Overall, these results indicate that activation with H_2SO_4 effectively reduces carbonate and organic

matter contents, thereby enhancing the physicochemical stability of the clay (Bessaha, 2016).

c. Moisture content

Table IV presents the results of the moisture content of raw and activated clays.

Table IV. Humidity Rate Results

Raw clay	Activated clay
3.60	2.72

The values reported in the table indicate relatively low moisture content. This can be attributed to the weakly hygroscopic nature of the clay. The measured moisture primarily corresponds to free water located between silicate layers, which is typically released at temperatures around 100°C.

A slight decrease in moisture content is observed following acid activation. This reduction can be explained by the chemical treatment applied to the clay. The reaction between the clay and the acid is exothermic, generating heat that promotes partial water evaporation. As a result, some of the initially retained water is lost during the activation process (Rezaiguia, 2017; Amirouche, 2011).

Recent thermogravimetric investigations provide additional insight into this behavior. They show that weakly adsorbed water is generally released at temperatures below 200°C, whereas more strongly bound water requires higher activation energies, which depend on the structural characteristics of the clay. In this regard, Lo Dico et al. (2024) demonstrated that fibrous clays such as sepiolite and palygorskite require significantly higher activation energies (160–190 kJ/mol) than laminar clays like montmorillonite and stevensite (80–100 kJ/mol). These findings are consistent with our observations, suggesting that acid activation reduces the fraction of strongly bound water. Consequently, the overall moisture content decreases, accompanied by modifications in the adsorption properties of the clay.

d. pH

The pH results of the raw and activated clays are presented in table V.

Table V. pH Results

Raw clay	6.22
Activated clay	4.12

The results indicate that the activated clay exhibits a more pronounced acidity than the raw material. This increase can be attributed to the higher concentration of exchangeable H^+ ions generated during the acid activation process. Such an enrichment in protonic sites significantly modifies the chemical behavior of the clay, influencing its adsorption capacity, its reactivity toward various compounds, and its interactions in both industrial and environmental contexts (Rezaiguia, 2017).

The pH values reported in Table VII further show that both raw and activated clays fall within the range of slightly acidic materials. This baseline acidity is consistent with that typically observed in naturally acidic soils, distinguishing them from neutral or alkaline sources. Acid activation intensifies this characteristic by removing exchangeable cations such as Ca^{2+}, Mg^{2+}, and Na^+ and replacing them with protons. This substitution increases the density of active sites and enhances the overall reactivity of the clay.

These observations are in agreement with previous studies. Ayati et al. (2022) reported that acid-activated smectite clays undergo a significant decrease in pH, accompanied by improved pozzolanic reactivity and binding capacity in cementitious systems. Similarly, Bahranowski et al. (2022) demonstrated that acid impregnation of Ca-bentonite, following thermal pretreatment, leads to a rapid exchange of Ca^{2+} ions with H_3O^+ species, stabilizing the protonated form of montmorillonite and resulting in a marked reduction in pH. More recently, Lo Dico et al. (2024) highlighted that combined thermal and chemical treatments modify both water binding and proton exchange mechanisms, thereby directly affecting the acidity and reactivity of clay materials.

e. Zero charge point

Table VI presents the initial pH and final pH of the raw and activated clays, which allowed us to find the pH at the zero charge point.

Table VI. PCN Results

pH_i(AB)	pH_f(AB)	pH_i(AA)	pH_f(AA)
3.41	5.32	3.24	4.22
6.23	7.45	6.15	7.67
9.42	8.61	9.23	8.53
12.1	11.13	12.18	9.88

Figure 4 and figure 5 show us the intersection of the lines to which corresponds the pH at the point of zero charge.

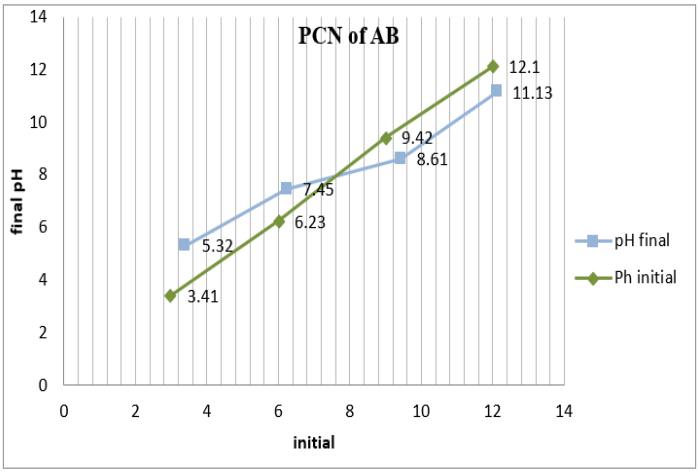

Figure 4. PCN of raw clays

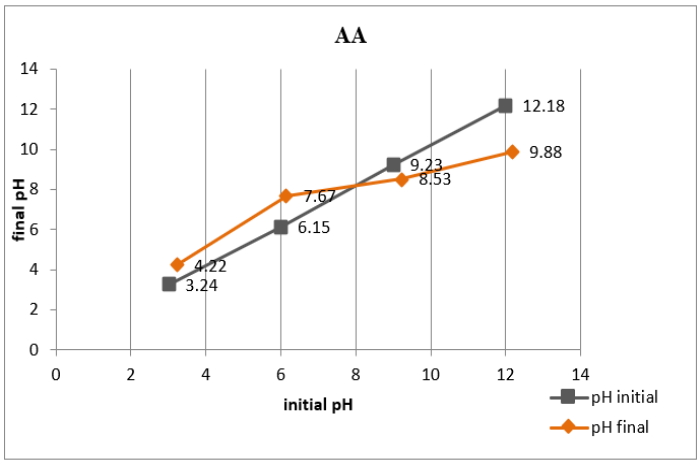

Figure 5. PCN of activated clays

From a practical perspective, the positive surface charge observed on both raw and activated clays carries several important implications.

f. Adsorption capacity

Surfaces bearing a positive charge tend to exhibit a strong affinity for negatively charged species, including phosphates, nitrates, and various organic anions. This behavior is well documented in environmental remediation studies, where clays are extensively used to remove anionic contaminants from aqueous systems (Kosmulski, 2009; Kosmulski, 2021; Madejová et al., 2006). More recent research further highlights that adjusting surface charge through acid activation can significantly enhance adsorption efficiency, particularly for heavy metals and dye molecules (Lo Dico et al., 2024).

g. Flocculation behavior

The electropositive character of the clay also promotes the neutralization of negatively charged colloidal particles. This facilitates aggregation, sedimentation, and overall clarification of suspensions. Such behavior is consistent with classical colloid science, in which the point of zero charge governs suspension stability and determines the tendency of particles to either remain dispersed or aggregate (Kosmulski, 2021).

h. Catalytic potential

Acid activation increases the number of protonated sites on the clay surface, which can enhance its catalytic performance. In heterogeneous catalysis, these proton-rich active sites are known to promote acid-catalyzed reactions, such as esterification and transesterification. Studies on sulfonated and thermally treated clays confirm that these modified surfaces can act as efficient catalytic centers (Madejová et al., 2006; Lo Dico et al., 2024).

However, excessively high pHPCN_{PCN}PCN values may also impose certain limitations. In strongly acidic environments, the surface can become saturated with protons, which may reduce its reactivity toward specific target species. In this context, careful optimization of activation conditions such as reaction time, temperature, and acid concentration appears essential. Fine-tuning these parameters allows for controlled adjustment of surface charge properties, making it possible to tailor the material to specific industrial or environmental applications. This perspective aligns with the conclusions of Kosmulski (2021), who emphasized that precise control of surface charge is a key factor in maximizing both adsorption efficiency and catalytic performance across varying pH conditions.

3. 2. Characterization of raw and activated clays

3.2.1. Chemical composition

The results of the chemical composition of raw and activated clays carried out by XRF are presented in table VII.

Table VII. Chemical Composition Results

Compounds	Test method	Unit	Raw clay	Activated clay
SiO2 - XRF	DIN EN 196-2:2019	%	73.87	77.75
Al2O3 - XRF	DIN EN 196-2:2013	%	12.00	10.77
Fe2O3 - XRF	DIN EN 196-2:2013	%	2.87	1.19
CaO-XRF	DIN EN 196-2:2013	%	2.80	3.01
MgO- XRF	DIN EN 196-2:2013	%	0.53	0.42
SO3 - XRF	DIN EN 196-2:2013	%	0.62	0.39
K2O- XRF	DIN EN 196-2:2013	%	0.34	0.30
Na2O .XRF	DIN EN 196-2:2013	%	0.83	0.81
P2O5 - XRF	DIN EN 196-2:2013	%	0.00	0.00
MnO2 .XRF	DIN EN 196-2:2013	%	0.00	0.00
TiO2 - XRF	DIN EN 196-2:2013	%	0.47	0.46
Total XRF - 1050 °C	DIN EN 196-2:2013	%	99.49	99.49

Chemical composition analysis indicates that the activated clay is predominantly composed of silica and alumina. The SiO_2/Al_2O_3 ratio increased from 6.16 in the raw clay to 7.22 after activation, reflecting a marked enrichment in free silica, mainly in the form of quartz. This trend is supported by a 3.88% increase in silica content following activation, accompanied by a decrease in Al_2O_3, Fe_2O_3, and MgO contents.

These changes can be attributed to the acid activation process, which selectively dissolves aluminum, iron, and magnesium from the octahedral layers of the clay structure. In contrast, silicon remains largely insoluble, leading to its relative enrichment. Such selective leaching mechanisms are well documented in recent studies on acid-treated clays, where the removal of structural cations is associated with an increase in silica content (Berhe et al., 2024; Madejová et al., 2024).

The resulting modifications in chemical composition have several implications for the physicochemical and mechanical behavior of the activated clay. The removal of octahedral cations tends to weaken structural cohesion, which may reduce plasticity while simultaneously enhancing porosity and surface reactivity (Abir, 2016). At the same time, silica enrichment contributes to an increase in specific surface area, thereby improving the material's capacity to adsorb both organic and inorganic contaminants. This observation is consistent with reported results for acid-activated bentonite and kaolinite systems (Berhe et al., 2024). In addition, acid treatment promotes the formation of reactive surface groups, particularly silanol functions, which can act as active sites in heterogeneous catalytic processes (Madejová et al., 2024).

Compared with previous studies, the degree of silica enrichment observed here appears relatively pronounced. For instance, Boudouara (2021) reported silica contents of approximately 27.52% in raw clay and 30.11% after activation with 1N H_2SO_4, while Berhe et al. (2024) described an increase from around 58% to higher values in Ethiopian bentonite. The more substantial enrichment obtained in the present work can likely be explained by the higher acid concentration employed, which enhances the dissolution of octahedral cations and consequently increases the relative proportion of silica.

3.2.2. Mineralogical composition

Table VIII presents the results of the mineralogical composition of raw and activated clays carried out by XRD.

Table VIII. Mineralogical composition results

Phases	Chemical formula	Unit	AB	AA
Oxides				
Anatase	TiO2	%	0.53	0.46
Goethite / Lepidocrocite	a-FeOOH / γ -FeOOH	%	2.40	0.84
Hematite	Fe2O3	%	0.53	0.44
Quartz	SiO2	%	**45.41**	**45.35**
Rutile	TiO2	%	0.57	0.61
Feldspars, amphiboles				
Albite/Anorthose (Alkaline Feldspar)	$(Na_{0.5}K_{0.5})AlSi_3O_8$	%	2.24	2.75
Microcline	$KAlSi_3O_8$	%	3.42	2.88
Clay minerals, micas				
Illite	$K_{0.5}(H3O)_{0.5}Al_2[(OH)_2\|AlSi_3O_{10}]$	%	**8.23**	**15.59**
Kaolinite	$Al_4[(OH)_8\|Si_4O_{10}]$	%	**34.59**	**29.98**
Carbonates				
Calcite	CaCO3	%	0.69	0.65
Dolomite	$CaMg(CO_3)_2$	%	0.46	0.19
Others				
Chlorite	$(Fe, Mg, Al)_6(Si, Al)_4O_{10}(OH)_8$	%	**0.76**	**0.19**
Pyrite	FeS_2	%	0.17	0.07
Total XRD			100.00	100.00

The X-ray diffraction (XRD) patterns obtained for both raw and acid-activated clay samples reveal the presence of kaolinite, chlorite, and illite as the main mineral phases. In both cases, kaolinite remains the dominant component, indicating that the acid treatment did not fully disrupt the layered aluminosilicate structure of the clay. This observation is consistent with recent studies on chemically activated kaolinitic clays, where moderate acid activation preserves the primary crystalline framework while inducing partial dealumination and structural rearrangement (Hazarika et al., 2024).

In the diffractograms (figures 6 and 7), the most intense peak is attributed to quartz, confirming the high

silica content previously identified by X-ray fluorescence (XRF) analysis. The predominance of quartz is characteristic of silica-rich clays and is commonly reported in acid-activated systems, as quartz exhibits strong resistance to acid dissolution compared with other aluminosilicate minerals. Recent work has shown that acid treatment preferentially alters octahedral clay structures while leaving crystalline silica phases largely unaffected, resulting in increased quartz peak intensity in XRD patterns (Hazarika et al., 2024).

A noticeable reduction in the relative abundance of kaolinite and chlorite is observed after activation, whereas the proportion of illite increases. These mineralogical changes can be explained by the selective leaching induced by sulfuric acid treatment (H_2SO_4, 3 N). Acid activation promotes the removal of structural cations such as Al^{3+}, Fe^{3+}, Mg^{2+}, and Ca^{2+}, leading to partial degradation of phases that are more sensitive to acidic conditions, including kaolinite and chlorite. In contrast, illite exhibits greater structural resistance under moderate acidity, which accounts for its relative enrichment. Similar trends were reported by Saed & Al-Mammar (2021), who observed a decrease in kaolinite and chlorite phases alongside improved adsorption performance in acid-treated mixed clays.

The decrease in kaolinite peak intensity further suggests partial alteration of hydroxyl-bearing octahedral layers, resulting in the formation of new pores and active adsorption sites. Acid activation is well known to enhance the physicochemical properties of clays by increasing specific surface area, expanding pore volume, and modifying surface functional groups. In line with this, recent studies have demonstrated that acid-activated kaolinite exhibits improved adsorption capacities toward heavy metals, dyes, and organic pollutants due to increased surface reactivity and the generation of additional active sites (Liu et al., 2024).

The relative increase in illite content may also contribute positively to the adsorption performance of the activated clay. Compared with kaolinite, illite possesses a higher cation exchange capacity (CEC), associated with its partially expandable layered structure and the presence of exchangeable interlayer cations. As a result, its enrichment after activation can enhance the retention of ionic species in aqueous environments. Comparable findings were reported by Saed & Al-Mammar (2021), who linked improved dye adsorption efficiency to mineralogical and surface modifications induced by acid activation.

The persistence of relatively high proportions of kaolinite and illite after treatment can be attributed to the moderate concentration of sulfuric acid used (H_2SO_4, 3 N). Recent studies indicate that such conditions allow for effective surface modification and partial dealumination without causing complete collapse of the crystalline structure. This balance is crucial, as it enables improvements in porosity, surface acidity, and adsorption performance while preserving structurally favorable mineral phases. In contrast, excessively concentrated acid solutions tend to induce extensive dissolution of aluminosilicate layers, leading to severe structural degradation and a consequent reduction in adsorption efficiency (Taxiarchou et al., 2025).

Overall, the XRD results demonstrate that acid activation induces significant mineralogical and structural modifications without fully destroying the clay framework. The reduction of kaolinite and chlorite, combined with the relative enrichment of illite and the persistence of quartz, indicates that sulfuric acid treatment enhances the physicochemical properties of the material. These changes are expected to improve adsorption behavior and broaden the potential applications of the activated clay in areas such as environmental remediation, catalysis, and wastewater treatment.

a. Raw Clay (AB) (Coupled TwoTheta/Theta)

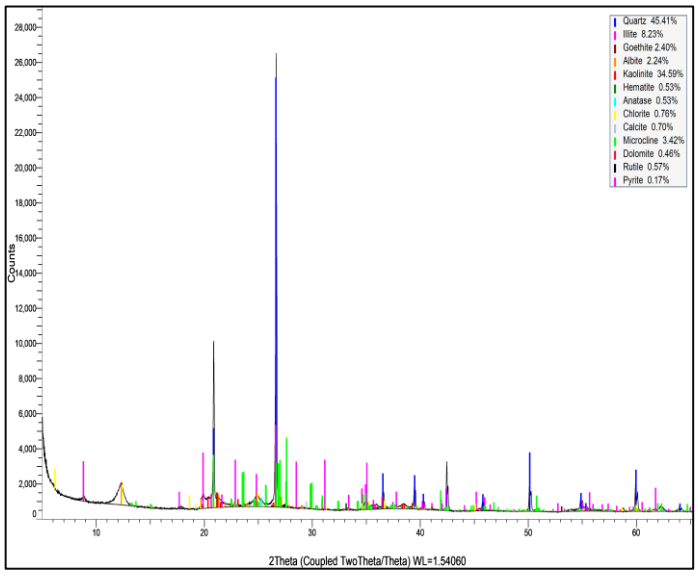

Figure 6. XRD spectrum of raw clays

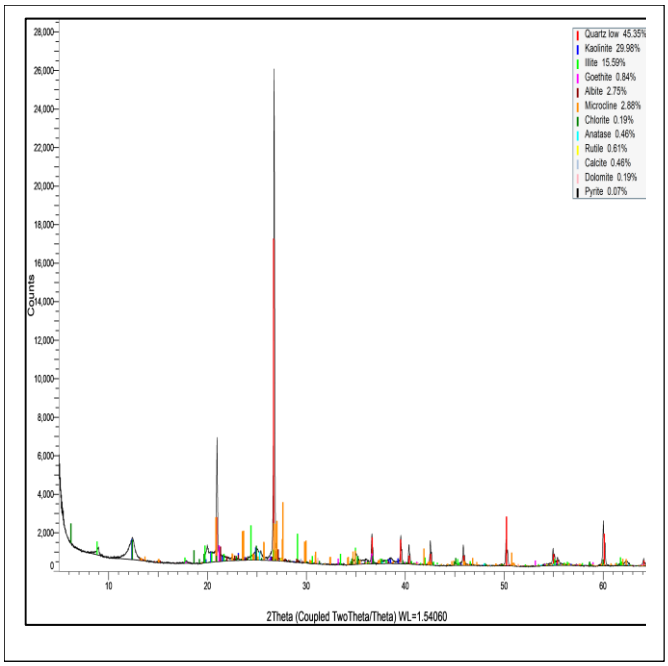

Figure 7. XDR spectrum of activated clay

3.3. Physicochemical parameters of oils

The results of the physicochemical analyses are given comparatively according to the treated, used and new oil.

3.3.1. Color

Table IX presents the results for color.

Table IX. Color Results

New oil	Used oil	treated oil
Brunette	Black	Black

The results show that the fresh oil exhibited a brownish coloration, whereas both the used and regenerated oils remained black (Parekh et al., 2025; Stan et al., 2018). The persistence of this dark color indicates that the treatment was not sufficient to fully remove oxidation products, suspended particles, and other chromophoric impurities responsible for the typical appearance of degraded oils (Islam et al., 2024; Ma et al., 2020).

However, color should be interpreted as a qualitative, macroscopic indicator rather than a definitive measure of regeneration efficiency (Ma et al., 2020). A reliable assessment of oil recovery must instead rely on standardized physicochemical parameters, such as viscosity, density, acidity, water content, and the extent of contaminant removal (Juraev et al., 2025; Ugwele et al., 2020; Islam et al., 2024).

3.3.2. Kinematic viscosity at 40°C and 100°C in cSt

Table X summarizes the kinematic viscosity of the new oil, used oil, and treated oil at 40°C and 100°C. At 40°C.

Table X. Kinematic viscosity results at 40°C and 100°C

Kinematic viscosity	New oil	Used oil	treated oil	boundaries
40°C	136.9	95.9	95.8	100-200 (ISO-VG)
100°C	14.1	0.01	7.4	13.5-14.5 (ISO-VG)

The results indicate that the fresh oil exhibits the highest viscosity, reaching 136.9 cSt, whereas both the used and treated oils display lower and nearly identical values (95.9 and 95.8 cSt, respectively). This decrease is consistent with the progressive degradation of the lubricating formulation during service. In particular, it reflects the depletion of viscosity-modifying additives and the alteration of the hydrocarbon matrix under combined thermal and oxidative stresses (Ugwele et al., 2020; Stan et al., 2018). In re-refining contexts, such variations in viscosity are commonly linked to additive consumption, the accumulation of oxidation by-products, and the formation of low-molecular-weight compounds, all of which contribute to a reduced resistance to flow at moderate temperatures (Islam et al., 2024; Parekh et al., 2025).

At 100°C, however, the reported kinematic viscosity of the used oil (0.01 cSt) is exceptionally low and does not correspond to physically realistic values for lubricating oils. This anomaly strongly suggests the presence of an experimental or data-processing error, potentially arising from incorrect unit conversion, transcription inaccuracies, or measurement artifacts. By contrast, the treated oil exhibits a viscosity of 7.4 cSt, indicating a partial recovery of its flow properties following treatment. This improvement can reasonably be attributed to the adsorption of polar degradation products, sludge precursors, and other destabilizing compounds by the clay used in the process, leading to the removal of species that adversely affect oil stability (Juraev et al., 2025; Stan et al., 2018).

Despite this improvement, the treated oil does not reach the reference viscosity of the fresh oil at 100°C (14.1 cSt). This suggests that the regeneration process, while effective to some extent, remains incomplete and does not fully restore the original rheological characteristics of the lubricant (Islam et al., 2024; Parekh et al., 2025).

3.3.3. Viscosity index

The results for the viscosity index are presented in table XI.

Table XI. Viscosity Index Results

New oil	Used oil	treated oil
98.4	-	23.3

The viscosity index results clearly indicate that the fresh oil maintains significantly better thermal stability than the treated sample. The reference oil exhibits a viscosity index of 98.4, whereas the treated oil shows a sharp decrease to 23.3. This substantial reduction suggests that, although the regeneration process led to some improvement, it did not fully restore the original temperature–viscosity relationship of the lubricant. As for the used oil, its viscosity index could not be reliably determined due to the anomalous viscosity value reported at 100°C, which renders the calculation invalid.

The low viscosity index observed for the treated oil reflects a partial recovery of properties rather than a complete restoration. While the treatment appears to have removed part of the contaminants and degradation products, the oil still exhibits pronounced deterioration in its rheological behavior. Such observations are consistent with findings reported in the literature on used-oil re-refining. Regeneration processes generally improve certain physicochemical characteristics, yet they rarely succeed in fully reconstituting the molecular structure of the base oil or reproducing the performance of a fresh lubricant. For instance, Islam et al. (2024) emphasized that, although re-refining enhances the quality of waste oil, complete recovery typically requires both efficient contaminant removal and additional upgrading steps. Similarly, Juraev et al. (2025) demonstrated that the final properties of regenerated oils strongly depend on the balance between acids and adsorbents, highlighting the process-dependent nature of regeneration outcomes.

The marked reduction in viscosity index can also be interpreted in light of known degradation mechanisms. During service, lubricating oils undergo several irreversible transformations, including additive depletion, polymer shear degradation, thermal cracking, and thermo-oxidative breakdown of viscosity-modifying agents. These processes collectively diminish the oil's ability to maintain stable viscosity as temperature increases. Studies by Stan et al. (2018) and Parekh et al. (2025) further confirm that, even when regeneration improves certain properties, the rheological stability of the treated oil often remains inferior to that of fresh oil if degraded fractions are not entirely removed or if the original formulation is not fully restored. In addition, Ugwele et al. (2020) demonstrated that regeneration efficiency is highly sensitive to operating conditions, with suboptimal parameters resulting in incomplete recovery of functional properties.

Overall, the viscosity index results point to partial regeneration rather than full restoration. Although the treated oil shows some improvement compared with the used sample, its very low viscosity index indicates insufficient thermal stability for performance equivalent to that of a new lubricant. Consequently, the regenerated oil should be regarded as only partially recovered. Further purification or upgrading steps would be necessary to approach the properties of the fresh oil.

3.3.4. Density

The density results are presented in table XII.

Table XII. Density Results

New oil	Used oil	treated oil	Limit
0.886	0.890	0.928	0.85-0.95 (SAE)

The density of the treated oil remains within the standard SAE range, indicating that it is still technically suitable for use, despite a slight increase following regeneration. This increase in density may be explained by the presence of residual fine clay particles, suspended solids, and high molecular weight compounds that were not fully removed during the treatment process. Such residual constituents can artificially elevate the measured density, suggesting that the regeneration process did not entirely restore the oil to its original condition.

These observations are consistent with findings reported in the literature on used oil re refining. The efficiency of regeneration processes largely depends on the ability of the adsorbent to effectively remove impurities and ensure adequate phase separation. When treatment conditions are not fully optimized, heavier fractions and solid residues may persist, leading to alterations in key physicochemical properties of the oil. Similar behavior has been documented in studies by Islam et al. (2024), Juraev et al. (2025), Parekh et al. (2025), Stan et al. (2018), and Ugwele et al. (2020), all

of whom emphasize the critical role of adsorbent performance and process control in achieving effective oil regeneration.

3.3.5. Flash point in °C

The flash point results presented in Table XV show a clear decrease from the new oil (234°C) to the used oil (98°C), indicating a substantial loss of thermal safety during service.

Table XIII. Flash Point Results

New oil	Used oil	treated oil	Boundaries
234	98	135	> 150 (ISO-VG)

This reduction is consistent with the formation of lighter volatile fractions generated during engine operation and oxidative degradation. These compounds tend to lower the temperature at which vapors become ignitable, thereby decreasing the flash point. After treatment, the flash point increases to 135 °C, indicating a partial removal of volatile compounds and degradation products through adsorption mechanisms.

This improvement aligns with findings reported in the literature, which show that regeneration processes can restore part of the oil's properties, although the treated product generally remains below the reference values of fresh oil (Ugwele et al., 2020; Parekh et al., 2025). It is therefore important to interpret the evolution of the flash point alongside other physicochemical parameters, as improvements in a single property or visual appearance do not necessarily reflect a complete restoration of lubricant quality (Ma et al., 2020).

Despite the observed increase, the flash point of the treated oil remains below the ISO VG threshold of 150 °C. This confirms that, while the regeneration process enhances certain properties, it does not fully recover the thermal stability required to match that of a new lubricant.

3.3.6. The pouring point in °C

The pour point results presented in table XIV show that the new oil has a value of -27°C, the used oil -12°C, and the treated oil -30°C.

Table XIV. Pour point results

New oil	Used oil	treated oil	Boundaries
-27	-12	-30	< -45 (ISO-VG)

The higher pour point observed for the used oil, compared with the fresh oil, reflects a deterioration in low-temperature fluidity. This behavior is consistent with the depletion of additives and the accumulation of degradation products during engine operation, both of which adversely affect flow properties at reduced temperatures.

Following treatment, the pour point decreases to −30 °C, indicating a clear improvement in low-temperature performance. This change suggests that the adsorption process using activated clay effectively removed part of the impurities responsible for flow resistance, particularly those that promote solidification or hinder molecular mobility under cold conditions.

Such results are consistent with findings reported in the literature, where re-refining processes are shown to partially restore the physicochemical characteristics of used oils. However, the extent of recovery remains limited and strongly dependent on the treatment method and the efficiency of the adsorbent employed (Islam et al., 2024; Juraev et al., 2025; Parekh et al., 2025). Similar studies have also demonstrated that regeneration improves low-temperature behavior primarily through the removal of contaminant species that interfere with fluidity. Nevertheless, the final performance of treated oils often.

5. Conclusion

This study investigated the regeneration of used engine oil through percolation using discs made of acid-activated red clay. Overall, the results indicate that the process achieved partial regeneration, with noticeable improvements in several physicochemical properties. However, the treated oil did not fully recover the characteristics of the fresh lubricant. In this respect, the method demonstrates clear potential as a low-cost and locally accessible purification approach, although it remains insufficient for complete restoration.

The characterization of the clay confirmed that acid activation substantially altered its properties and enhanced its performance as an adsorbent. The treated clay exhibited lower moisture content and increased acidity, alongside a modified chemical composition marked by higher silica content and reduced concentrations of certain impurity-related oxides. Together, these changes point to the development of a more reactive surface, capable of effectively adsorbing polar compounds, degradation products, and other contaminants present in used oil.

Regarding the treated oil, several improvements were observed. The flash point increased compared with the used oil, indicating a reduction in volatile components. Similarly, the pour point decreased, reflecting improved fluidity at low temperatures

following treatment. The density of the regenerated oil remained within the acceptable SAE range, although it was higher than that of the fresh oil, suggesting incomplete removal of retained solids and heavy fractions. In addition, both kinematic viscosity and viscosity index showed only partial recovery, confirming that while improved the treated oil still falls short of the performance level of the fresh lubricant.

The color of the oil remained unchanged after treatment, further illustrating that visual appearance alone cannot be considered a reliable indicator of regeneration efficiency. Overall, these findings highlight the technical potential of acid-activated red clay as an adsorbent for used-oil regeneration. Its adsorption properties clearly contribute to improving oil quality, yet the process remains incomplete.

Further progress will depend on optimizing key parameters, including activation conditions, filter configuration, and operating variables, in order to enhance purification efficiency and approach the properties of fresh oil more closely. Future work should also address the mechanical stability of the clay discs and investigate alternative system designs such as packed columns while comparing the performance of activated red clay with other adsorbent materials. Finally, more extensive experimental replication and comprehensive physicochemical analyses would strengthen the robustness of the results and support potential scale-up toward practical or industrial applications.

Acknowledgments

The authors would like to express their sincere gratitude to the Department of Chemistry, Faculty of Sciences, University of Kinshasa, for providing the laboratory facilities and technical support necessary for the completion of this work.

Special thanks are extended to the staff of SEP-CONGO for their assistance in carrying out the physicochemical analyses of the oil samples, as well as to the CILU industrial cement laboratory for facilitating the XRD and XRF analyses.

The authors also acknowledge I-Engineering DRC for supplying the used oil samples and for their collaboration during the experimental phase.

Funding

This research did not receive any specific grant from funding agencies in the public, commercial, or not-for-profit sectors.The work was carried out using institutional resources and personal contributions from the authors.

Conflict of interest

The authors declare that they have no conflict of interest regarding the publication of this paper.

Ethical considerations

This study did not involve human participants or animals.

All experimental procedures were conducted in accordance with standard laboratory practices and environmental safety regulations.

The collection and handling of used lubricating oils were carried out in compliance with environmental protection guidelines.

Author contributions

I.K.M.: Conceptualization, methodology, experimental work, data analysis, and manuscript drafting.

H.K.M.: Experimental investigations and data collection.

T.K.K.: Data interpretation and validation of results.

K.M.T.: Scientific supervision and critical revision of the manuscript.

A.K.M.: Laboratory analyses and technical support.

J.M.: Data processing and statistical analysis.

E.K.K.: Analysis and interpretation of X-ray diffraction (XRD) spectra and contribution to the discussion of the associated results.

J.M.K.: Experimental assistance and materials preparation.

B.M.N: Data curation, preparation of figures and tables, and assistance in drafting the results section.

N.N.C: Environmental risk assessment, interpretation of used oil disposal, and contribution to sustainability perspectives in the manuscript

M.K.M.: Environmental analysis and interpretation.

J.K.N.: Project administration, supervision, and final validation of the manuscript.

Orcid of authors

Mulumba K.I.: https://orcid.org/0009-0000-8053-5184;

Malengila K.H.: https://orcid.org/0009-0003-0209-1268;

Kashishi K.T.: https://orcid.org/0009-0000-6597-7371;

Taba M.K.: https://orcid.org/0000-0002-2784-9333;

Muabu K.A.: https://orcid.org/0009-0005-2343-2310;

Muyumba J.: https://orcid.org/0000-0002-7595-4859;

Kapuya K.E.: https://orcid.org/0009-0006-9129-4359;

Kamwiziku M.J.: https://orcid.org/0009-0001-6506-8730;

Mputu K.M.: https://orcid.org/0009-0009- 1654-7020;

Bolangongo M.N: https://orcid.org/0009-0005-0005-3312

Ngoyi N.C: https://orcid.org/0009-0003- 2282-5820;

Ntumba K.J.: https://orcid.org/0009-0003-1914-3741.

References

Abir, A. (2016). *Clay activation: Modes and structural modifications* [Master's thesis, National Polytechnic School].

Amirouche, L. (2011). *Study of the sorption capacity of copper (II), zinc (II), and polyphenols by bentonites under microwave irradiation* [Master's thesis, Mouloud Mammeri University of Tizi-Ouzou].

Amrane, K., & Boubekeur, S. (2017). *Chemical regeneration of used dielectric oils using raw bentonite from Maghnia* [Master's thesis, Djilali Bounaama University of Khemis Miliana].

Anisuzzaman, S. M., & Jumadil, N. S. (2024). Used lubricating oil treatment using acid activation clay as adsorbent for oil recovery. *Borneo Science Journal, 45*(2), 1–12. https://doi.org/10.51200/bsj.v45i2.5880

Armioni, D. M., Rațiu, S. A., Benea, M. L., & Puțan, V. (2024). Overview on the environmental impact of used engine oil. *Journal of Physics: Conference Series, 2927*(1), Article 012007. https://doi.org/10.1088/1742-6596/2927/1/012007

Ayati, B., Newport, D., Wong, H., & Christophe, C. (2022). Acid activated smectite clay as pozzolanic supplementary cementitious material. *Cement and Concrete Research, 162*, Article 106969. https://doi.org/10.1016/j.cemconres.2022.106969

Bahranowski, K., Klimek, A., Gaweł, A., Olejniczak, Z., & Serwicka, E. M. (2022). Rehydration driven acid impregnation of thermally pretreated Ca-bentonite—Evolution of the clay structure. *Materials, 15*(6), Article 2067. https://doi.org/10.3390/ma15062067

Bennoui, S. A., & Haleche, S. (2021). *Regeneration of used engine oils by acid treatment and adsorption* [Master's thesis, University of Blida 1].

Berhe, M. T., Gebreyohannes, G., Cheru, M. S., & Weldehans, M. G. (2024). Characterization of acid activation of bentonite clay of Hadar, Afar, Ethiopia. *Advances in Materials Science and Engineering*, Article 6413786. https://doi.org/10.1155/2024/6413786

Bessaha, F. (2016). *Thermal and chemical modification and application of a 1:1 clay for dye co-adsorption* [Doctoral thesis, Abdelhamid Ibn Badis University of Mostaganem].

Boudouara, N. (2021). *Application of modified clays for pollution control* [Doctoral thesis, Mustapha Stambouli University of Mascara].

Cabrera Escobar, M., González Martínez, J., López Ramírez, A., & Fernández Torres, P. (2026). Recycling of used lubricating oils: Environmental and economic perspectives. *Recycling, 11*(2), 145–160. https://doi.org/10.3390/recycling11020145

Dawood, I., Zyoud, A. H., Zyoud, S., Amireh, A., Zyoud, S. H., & Kim, T. W. (2025). Sustainable water treatment using thermally stable natural clay: Dual adsorption–thermolysis approach for organic pollutants and nitrate removal. *Scientific Reports, 15*, Article 29888. https://doi.org/10.1038/s41598-025-29888

Derafa, G. (2014). *Synthesis and characterization of modified montmorillonite: Application to the adsorption of cationic dyes* [Master's thesis, Ferhat Abbas University Sétif 1].

Dodoo, D., Appiah, G., Acquaah, G., & Dodoo, G., Jr. (2023). Fixed bed column study for the remediation of the bauxite liquid residue using acid activated clays and natural clays. *Heliyon, 9*(3), Article e14310. https://doi.org/10.1016/j.heliyon.2023.e14310

Fouzia, B. (2015). *Zinc adsorption by raw and activated bentonite* [Master's thesis, National Polytechnic School].

Ghafar, A. H., Radwan, E. K., & El-Wakeel, S. T. (2020). Removal of hazardous contaminants from water by natural and zwitterionic surfactant-modified clay. *ACS Omega, 5*(17), 10042–10052. https://doi.org/10.1021/acsomega.0c00834

Gorączko, A., & Topoliński, T. (2020). Particle size distribution of natural clayey soils: A discussion on the use of laser diffraction analysis (LDA). *Geosciences, 10*(2), Article 55. https://doi.org/10.3390/geosciences10020055

Grema, A. S., Idriss, I. M., Alkali, A. N., Ahmed, M. M., & Iyodo, H. M. (2021). Production of clay-based ceramic filter for water purification. *European Journal of Engineering and Technology Research*. https://doi.org/10.24018/ejers.2021.6.7.2623

Hazarika, A., Huang, L., & Babaahmadi, A. (2024). Characterisation, activation, and reactivity of heterogenous natural clays. *Materials and Structures, 57*, Article 68. https://doi.org/10.1617/s11527-024-02335-9

Heiri, O., Lotter, A. F., & Lemcke, G. (2001). Loss on ignition as a method for estimating organic and carbonate content in sediments: Reproducibility and comparability of results. *Journal of Paleolimnology, 25*(1), 101–110. https://doi.org/10.1023/A:1008119611481

Al Zubaidi, I., Al Tamimi, A., & Al-Zubaidi, M. (2021). Applications of de-oiling and reactivation of spent clay adsorbents for oil and effluent treatment. *Chemical Engineering Journal Advances, 15*, Article 100452. https://doi.org/10.1016/j.cengjadv.2023.100452

Islam Sazzad, M. R., Rahman, M., Hassan, T., Al Rifat, A., Al Mamun, A., Adib, A. R., Meraz, R. M., & Ahmed, M. (2024). Advancing sustainable lubricating oil management: Re-refining techniques, market insights, innovative enhancements, and conversion to fuel. *Heliyon, 10*(20), Article e39248. https://doi.org/10.1016/j.heliyon.2024.e39248

Juraev, T. E., Ismailov, O., Yakubov, Y. Y., & Auesbaev, A. U. (2025). Investigation of the physicochemical properties of recovered oil by determining the optimal amounts of acids and adsorbents in the used oil recycling process. *Chemical Problems*, (4).

Khan, S., Ajmal, S., Hussain, T., & Rahman, M. U. (2023). Clay based materials for enhanced water treatment: Adsorption mechanisms, challenges, and future directions. *Journal of Umm Al-Qura University for Applied Sciences, 11*, 219–234. https://doi.org/10.1007/s43941-023-00034-1

Khole, M. S., Tupe, S. K., & Sayyad, S. (2023). Estimating soil moisture content of bare soil using oven drying method. *International Journal of Scientific Research in Science and Technology*.

Kosmulski, M. (2009). *Surface charging and points of zero charge* (1st ed.). CRC Press. https://doi.org/10.1201/9781420051896

Kosmulski, M. (2021). The pH of zero point of charge: Review of 50 years of research. *Advances in Colloid and Interface Science, 294*, Article 102486. https://doi.org/10.1016/j.cis.2021.102486

Liu, T., Li, X., Wang, H., et al. (2024). Reconstructing kaolinite compounds for remarkably enhanced adsorption of Congo red. *Molecules, 29*(9), Article 2121. https://doi.org/10.3390/molecules29092121

Lo Dico, G., Lisuzzo, L., Carcelén, V., Cavallaro, G., & Haranczyk, M. (2024). Thermogravimetric analysis of moisture in natural and thermally treated clay materials. *Materials, 17*(10), Article 2231. https://doi.org/10.3390/ma17102231

Ma, J., Ruan, S., Hu, J., Sun, Y., Fei, Y., Jiang, X., Dong, S., Chen, T., & Wu, N. (2020). The intrinsic relationship between color variation and performances of the deteriorated aviation lubrication oil. *Journal of Industrial and Engineering Chemistry, 92*, 88–95. https://doi.org/10.1016/j.jiec.2020.08.023

Madani, A. (2008). *Contribution to the characterization and regeneration of used engine oils by percolation* [Master's thesis, National Polytechnic School].

Madejová, J., & Pálková, H. (2024). Review of the application of infrared spectroscopy in studies of acid-treated clay minerals. *Clays and Clay Minerals, 72*, Article e30. https://doi.org/10.1017/cmn.2024.24

Madejová, J., Jankovič, L., & Komadel, P. (2006). Identification of phases in thermally treated kaolinite by infrared spectroscopy and thermogravimetry. *Clay Minerals, 41*(4), 731–741. https://doi.org/10.1180/0009855064140217

Mishra, A., Mishra, S., & Patel, R. (2025). Hydrocarbon pollution and remediation strategies

for lubricating oils. *Environmental Science and Pollution Research*, *32*(5), 6789–6802. https://doi.org/10.1007/s11356-025-17890-2

Negasa, B., Alemu, T., Bekele, G., & Tadesse, M. (2025). Characterization of recycled lubricating oils using GC-MS and FTIR. *Scientific Reports*, *15*, Article 11234. https://doi.org/10.1038/s41598-025-11234-7

Osman, A. A., Gad Allah, M. A., & El Sheikh, A. H. (2021). Optimization of acidic activation conditions for natural clay and its application in waste oil bleaching. *Egyptian Journal of Chemistry*, *64*(10), 5167–5179. https://doi.org/10.21608/ejchem.2021.81234

Parekh, K., Gaur, R., & Shahabuddin, S. (2025). Re-refining used oil using rosin: A new approach for recycling waste engine oil. *Environmental Progress & Sustainable Energy*, *44*(6). https://doi.org/10.1002/ep.70072

Ravelomanantsoa, S. (2015). *Contribution to the valorization of used motor oils* [Master's thesis, Higher Polytechnic School].

Rezaiguia, W. (2017). *Removal of methylene blue by adsorption on natural and treated kaolin* [Master's thesis, Larbi Ben M'hidi University, Oum El Bouaghi].

Sabadash, V., Ivanova, N., & Petrenko, O. (2024). Adsorption of oil products by natural and modified sorbents. *Clean Technologies and Environmental Policy*, *26*(3), 455–468. https://doi.org/10.1007/s10098-024-02345-1

Saed, S. A., & Al-Mammar, D. E. (2021). Influence of acid activation of a mixture of illite, kaolinite, and chlorite clays on the adsorption of methyl violet 6B dye. *Iraqi Journal of Science*, *62*(6), 1761–1778. https://doi.org/10.24996/ijs.2021.62.6.2

Sarkar, B., Rusmin, R., Ugochukwu, U. C., Mukhopadhyay, R., & Manjaiah, K. M. (2019). Modified clay minerals for environmental applications. In B. Sarkar, R. Rusmin, U. C. Ugochukwu, R. Mukhopadhyay, & K. M. Manjaiah (Eds.), *Modified clay and zeolite nanocomposite materials* (pp. 1–25). Elsevier.

Sarkar, S., Banerjee, R., Chatterjee, P., & Das, K. (2023). Low cost adsorbents for regeneration of used lubricating oils. *Journal of Material Cycles and Waste Management*, *25*(4), 1890–1902. https://doi.org/10.1007/s10163-023-01567-9

Sarkar, S., Datta, D., Deepak, K. S., Mondal, B. K., & Das, B. (2023). Comprehensive investigation of various re-refining technologies of used lubricating oil: A review. *Journal of Material Cycles and Waste Management*, *25*, 1935–1965. https://doi.org/10.1007/s10163-023-01562-7

Sorrentino, G., Chellappah, K., & Biscontin, G. (2025). Understanding clogging mechanisms in filter media: An integration of laboratory findings and theoretical perspectives. *Separation and Purification Technology*, *330*, Article 130602. https://doi.org/10.1016/j.seppur.2024.130602

Stan, C., Andreescu, C., & Toma, M. (2018). Some aspects of the regeneration of used motor oil. *Procedia Manufacturing*, *22*, 709–713. https://doi.org/10.1016/j.promfg.2018.03.102

Taxiarchou, M., Tsakiri, D., & Douni, I. (2025). The impact of pH on the pore and structural characteristics of acid-modified bentonites in oxalate solutions. *Minerals*, *15*(3), Article 257. https://doi.org/10.3390/min15030257

Touir, I. F. Z., & Taleb, S. (2019). *Regeneration of Askarel oil* [Master's thesis, Mohamed Boudiaf University of M'sila].

Ugwele, F. O., Aninwede, C. S., Chime, T. O., Asadu, O. C., & Innocent, S. (2020). Application of response surface methodology in optimizing the process conditions for the regeneration of used mobil oil using different kinds of acids. *Heliyon*. https://doi.org/10.1016/j.heliyon.2020.e05062

Wang, Y., Xu, H., Gao, L., Yan, M., Duan, H., & Song, C. (2019). Regeneration of spent lubricant refining clays by solvent extraction. *Journal of Chemistry*. https://doi.org/10.1155/2019/1234567

Zahaf, F. (2017). *Structural study of modified clays applied to pollutant adsorption* [Doctoral thesis, Mustapha Stambouli University of Mascara].

Zhang, J., Li, Y. H., & Chen, X. (2022). Evaluation of loss on ignition method for organic matter determination in agricultural soils. *Soil Science Society of America Journal*, *86*(3), 456–468. https://doi.org/10.1002/saj2.20234